

# Dynamics of a tight-binding ring threaded by time-periodic magnetic flux

W. H. Hu and Z. Song\*

*School of Physics, Nankai University, Tianjin 300071, China*

(Received 17 May 2011; published 9 November 2011)

We analytically study the effects of periodically alternating magnetic fields on the dynamics of a tight-binding ring. It is shown that an arbitrary quantum state can be frozen coherently at will by the very frequent square-wave field as well as the monochromatic-wave field when the corresponding optimal amplitudes are taken. Numerical simulations show that the average fidelity depends on not only the system parameters, but also the features of the quantum state. Moreover, taking the initial zero-momentum Gaussian wave packets as examples, we show the dependence of the threshold frequency on the width of the packet for the given average fidelities. These observations provide a means to perform the quantum-state engineering.

DOI: [10.1103/PhysRevA.84.052310](https://doi.org/10.1103/PhysRevA.84.052310)

PACS number(s): 03.67.-a, 03.75.Lm

## I. INTRODUCTION

Coherent quantum-state storage and transfer via a coupled qubit system is an important problem in the emerging area of quantum-information processing (QIP). One of the promising methods of quantum-state transfer is the employment of a solid-state data bus with minimal spatial and dynamical control over the on-chip interactions between qubits [1–7]. However, small imperfections in receiving a quantum state and storing it coherently can seriously affect the fidelity of QIP. Stopping and freezing a flying qubit within a region of the data bus is a tool for this task. It has been proposed that a coupled-cavity-array system exhibits the possibility of an all-optical coherent control of light [8–11]. The dynamical control includes an adiabatic scheme, under which the quantum state is fixed on the superposition of the instantaneous eigenstates when the Hamiltonian varies slowly, and bang-bang control techniques, by means of a dynamical control field, at averaging to cease the unwanted evolution of the state.

Dynamical decoupling (DD) is a well-established paradigm of bang-bang control techniques, which employs a specially designed sequence of control pulses applied to the qubits in order to negate the coupling of the central spins to their environment [12]. Moreover, the quantum Zeno effect has been proposed as a strategy to protect coherence [13,14]. Recently, it has been proposed that a periodically driven potential can suppress the tunneling between adjacent sites in a lattice [15,16]. In this paper, we will pay attention to a fundamental aspect of QIP and generally study the influence of periodically alternating magnetic fields on the dynamics of a quantum state on a tight-binding ring. We consider the dynamics of the states in a tight-binding ring system that is pierced by a time-periodic magnetic flux,  $\Phi(t) = \Phi_0 + \Phi_A f(\omega t)$ , with the angular frequency  $\omega$ . We investigate the impact that the amplitude and frequency of the flux might have on the efficacy of the quantum control. We focus on the suppression of the evolution through a bang-bang control procedure, and study how the occurrence of a controlling field modifies the effectiveness of the control procedure. Our analysis is focused on the behavior of the fidelity of the evolved state with respect to the initial state, which has been employed to measure the efficiency of quantum-state transfer. We will

show that the time evolution of a state in such a time-dependent Hamiltonian can then be treated as an adiabatic process without any approximation. Then analytical results can be obtained, which should give more insight into quantum measurement and control. Additionally, this scheme can be applied to a neutral-particle system by torsional oscillation.

In Sec. II, we derive a general formalism for such a time-dependent system. We further introduce the expressions for the time-averaged fidelity, thus completing the description of the controllability of the systems for the quantum states. Sections III and IV are devoted to the applications of the formalism. These include a detailed treatment and computation of the time evolutions of typical initial states under the square and monochromatic time-periodic flux, respectively. Final conclusions and discussions are presented in Sec. V.

## II. MODEL AND GENERAL FORMALISM

In this section, we present the charged-particle model under consideration: a simple tight-binding model in an external magnetic field. Here, the particle-particle interaction is ignored for simplicity. Our approach is based on our previous work in Ref. [17], where we have proposed a scheme for quantum-state transfer. It employed a loop enclosing a static magnetic flux to control the speed of a wave packet. Another basic operation for the quantum-state engineering is coherently freezing a state on demand. For instance, quantum-information processing requires transferring, stopping, and freezing a flying qubit within a region of the data bus. In Ref. [17], we studied how to move a Gaussian wave packet at a certain speed on demand by a static magnetic flux. In this work, we aim at employing the same system with a periodically alternating flux for freezing a wave packet. By combining the two schemes, one can accomplish the task of “coherent storage and transfer” of a quantum state. Here we will generalize this description of the system in Ref. [17] by allowing for an additional time-periodic flux. We restrict our attention to the influence of the applied periodically alternating field on the dynamics of the particles.

Consider a ring lattice with  $N$  sites threaded by a magnetic field, as illustrated schematically in Fig. 1. The Hamiltonian of the corresponding tight-binding model,

$$H(t) = -J \sum_{j=1}^N (e^{i2\pi\Phi(t)/N} a_j^\dagger a_{j+1} + \text{H.c.}), \quad (1)$$

\*songtc@nankai.edu.cn

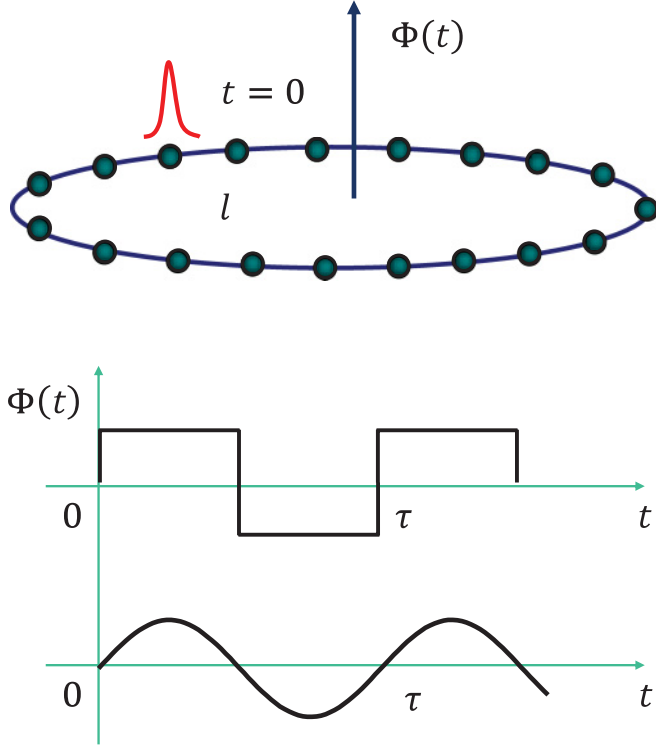


FIG. 1. (Color online) The schematic illustration for a tight-binding ring threaded by a time-periodic magnetic field. The time-dependent flux for demonstrating the influence on the evolution of a quantum state is in two types: square and monochromatic waves, respectively, with amplitude  $\phi_A$  and period  $\tau$ .

depends on the magnetic flux through the ring in units of the flux quantum,  $\Phi_0 = h/e$ . Here  $a_j^\dagger$  is the creation operator of a particle at the  $j$ th site with the periodic boundary condition  $a_{N+1} = a_1$ . The flux does not exert force on the Bloch electron, but can change the local phase of its wave function due to the Aharonov-Bohm (AB) effect. Note that the particle is not restricted to be either fermion or boson.

By taking the transformation

$$a_j = \frac{1}{\sqrt{N}} \sum_k e^{ikj} a_k, \quad (2)$$

where  $k = 2\pi n/N$ ,  $n \in [1, N]$ , the Hamiltonian can be readily written as

$$H = -2J \sum_k \cos[k + \phi(t)] a_k^\dagger a_k, \quad (3)$$

with  $\phi(t) = 2\pi \Phi(t)/N$  and the corresponding eigenstates in the form of

$$|k\rangle = \frac{1}{\sqrt{N}} \sum_j e^{ikj} |j\rangle. \quad (4)$$

Note that the time-dependent Hamiltonian possesses fixed eigenstates, while the flux solely affects the eigenvalues. It will be crucial to employ such a setup to investigate the control of a quantum state due to the rareness of the exact solutions to a time-dependent Hamiltonian. The evolution of an arbitrary state under the Hamiltonian  $H$  is dictated by the unitary operator  $U(t', t) = \exp(-i \int_t^{t'} H dt'')$ , which yields

the propagator represented in the momentum and spatial eigenstates as

$$\begin{aligned} U_{k'k}(t', t) &= \langle k' | U(t', t) | k \rangle = e^{i2Jf_k(t', t)} \delta_{kk'}, \\ U_{j'j}(t', t) &= \langle j' | U(t', t) | j \rangle \\ &= \frac{1}{N} \sum_k e^{ik(j'-j)} e^{i2Jf_k(t', t)}, \end{aligned} \quad (5)$$

where

$$f_k(t', t) = \int_t^{t'} \cos[k + \phi(t'')] dt''. \quad (6)$$

We note that the propagator is in diagonal form in  $k$  space.

In general, one employs the fidelity

$$F(t) = |\langle \psi(0) | U(t, 0) | \psi(0) \rangle| \quad (7)$$

to characterize the relation between the target state and the evolved state at time  $t$ . However, when  $\phi(t)$  is a periodic function,  $F(t)$  should be oscillating. Thus the long-time average will be appropriate as a measure for the deviation from the original state.

The average fidelity is defined as

$$\begin{aligned} \bar{F} &= \lim_{T \rightarrow \infty} \frac{1}{T} \int_0^T F(t) dt \\ &= \lim_{T \rightarrow \infty} \frac{1}{T} \int_0^T \left| \sum_k |c_k|^2 e^{i2Jf_k(t)} \right| dt, \end{aligned} \quad (8)$$

where

$$c_k = \langle k | \psi(0) \rangle.$$

In this paper, we focus on the case of periodic  $\phi(t)$  with a period of  $\tau$ ,

$$\phi(t) = \phi(t + \tau). \quad (9)$$

In the following sections, we will apply the general formalism to the cases of square and monochromatic waves for the following reasons: The square-wave case is a demonstrative example since it is the simplest model to calculate. The exact solution for this particular case is helpful to clearly present the main idea of the scheme without involving much more complicated calculations. And the monochromatic-wave case is a more practical situation. We will argue that the quantum-state freezing can be achieved by the high-frequency alternating flux when its amplitudes  $\Phi_A$  are optimal.

### III. SQUARE WAVE

Let us begin the discussion with the simplest case: the flux is in the form of

$$\phi(t) = \phi_0 + \phi_A \text{sgn}[\sin(\omega t)], \quad (10)$$

where  $\omega = 2\pi/\tau$  is the angular frequency and  $\text{sgn}$  indicates the sign function. It is a toy model that demonstrates how, in principle, the periodic alternating flux can prevent a quantum state from spreading. The Hamiltonian can be diagonalized as

$$H = -2J \sum_k \varepsilon_k(t) a_k^\dagger a_k, \quad (11)$$

$$\varepsilon_k(t) = \cos\{k + \phi_A \text{sgn}[\sin(\omega t)]\}, \quad (12)$$

where we absorbed  $\phi_0$  into  $k$  by  $k \rightarrow k - \phi_0$  for the sake of simplicity. Then we have

$$\overline{F}(\tau) = \lim_{T \rightarrow \infty} \frac{1}{T} \int_0^T \left| \sum_k |c_k|^2 \exp \left[ i2J \int_0^t \varepsilon_k(t') dt' \right] \right| dt. \quad (13)$$

Obviously, it is hard to get the analytical expression of  $\overline{F}(\tau)$ . However, one can get insight into the influence of the square wave on a quantum state from the following analysis. During each interval, with the flux being static, the dynamics of the quantum states in such a situation has been discussed in Ref. [17]. In particular, for  $\phi_A = \pi/2$ , the corresponding Hamiltonians are

$$H(t) = \begin{cases} H_+, & \text{sgn}[\sin(\omega t)] > 0 \\ H_-, & \text{sgn}[\sin(\omega t)] < 0, \end{cases} \quad (14)$$

with

$$H_{\pm} = \pm 2J \sum_k \sin k a_k^\dagger a_k. \quad (15)$$

Then the dynamics on the successive time intervals  $[t, t + \tau/2]$  and  $[t + \tau/2, t + \tau]$  are time-reversal processes to each other, i.e.,

$$\begin{aligned} U_{k'k}(t + \tau/2, t) &= U_{k'k}(t + \tau, t) U_{k'k}(t + \tau/2, t + \tau) \\ &= U_{k'k}^{-1}(t + \tau, t + \tau/2), \\ t &\in [0, \tau/2], \end{aligned} \quad (16)$$

which leads to

$$|\psi(t)\rangle = |\psi(t + \tau)\rangle \quad (17)$$

for an arbitrary state. Then, after a period of time  $\tau$ , any state will go back to its initial state, i.e.,

$$F(t) = F(t + \tau), \quad F(n\tau) = 1. \quad (18)$$

For small  $\tau$ , the evolved state should not leave its initial state so far at any time. Intuitively, in the limit of  $\tau \rightarrow 0$ , the initial state may be frozen at its initial position. Actually, the periodicity of  $|\psi(t)\rangle$  admits

$$\overline{F} = \frac{2}{\tau} \int_0^{\tau/2} \left| \sum_k |c_k|^2 e^{i2J \sin kt} \right| dt, \quad (19)$$

and

$$\lim_{\tau \rightarrow 0} \overline{F} \simeq \lim_{\tau \rightarrow 0} \frac{2}{\tau} \int_0^{\tau/2} \left| 1 + i2Jt \sum_k |c_k|^2 \sin k \right| dt = 1, \quad (20)$$

due to  $\sum_k |c_k|^2 = 1$ ,  $|\sum_k |c_k|^2 \sin k| < 1$ . We conclude that an arbitrary state can be frozen at will when the frequency is sufficient high. Particularly, in the case of  $|c_k|^2$  being symmetrical about  $k = 0$ , we simply have

$$\overline{F} = \frac{2}{\tau} \int_0^{\tau/2} \left| \sum_k |c_k|^2 \cos(2Jt \sin k) \right| dt, \quad (21)$$

and for small  $\tau$  ( $\tau \ll J^{-1}$ ), it has the form of

$$\overline{F} \simeq 1 - \frac{1}{6} J^2 \tau^2 \sum_k |c_k|^2 \sin^2 k. \quad (22)$$

Obviously,  $\sum_k |c_k|^2 \sin^2 k$  determines the speed of convergence: the more the contribution of  $|c_k|^2$  to zero  $k$ , the faster the convergence speed. In the following, we estimate the convergence speed of a specific state. A Gaussian wave packet with central momentum  $k_0$  can be expressed in the form of

$$c_k = \lambda \exp \left[ -\frac{\alpha^2}{2} (k - k_0)^2 \right], \quad (23)$$

where

$$\lambda^{-1} = \sqrt{\sum_k \exp[-\alpha^2 (k - k_0)^2]}$$

is the normalization factor and equal to  $\sqrt{N/(2\sqrt{\pi}\alpha^2)}$  for large  $N$ . Here  $\alpha$  determines the width of the wave packet. We consider such a state with  $k_0 = 0$  as the initial state. For large frequency  $\nu = 1/\tau$ , we have the frequency dependence of the average fidelity as

$$\overline{F} - 1 \simeq -\frac{J^2}{12\nu^2} [1 - e^{-\frac{1}{\alpha^2}}]. \quad (24)$$

Then, for the given initial state, we have evaluated the threshold frequency as

$$\nu_c = J \sqrt{\frac{1 - e^{-\alpha^{-2}}}{12(1 - \overline{F}_c)}}, \quad (25)$$

from which one can obtain the control of the quantum state with fidelity  $\overline{F}_c(\tau)$ . We plot Eq. (25) in Fig. 2, which shows that the threshold frequency increases rapidly when the width of the state gets narrow.

So far, our investigation is carried out analytically for a particular case of  $\phi_A = \pi/2$ . It can be seen that the mechanism of the perfect quantum-state freezing, expressed as Eq. (18), is the periodicity of the evolved wave function, given by Eq. (17), arising from the amplitude  $\phi_A = \pi/2$ . It is worthwhile to investigate what happens for other values of  $\phi_A$  and finite frequencies. In the following, we will perform a series of numerical simulations from several aspects.

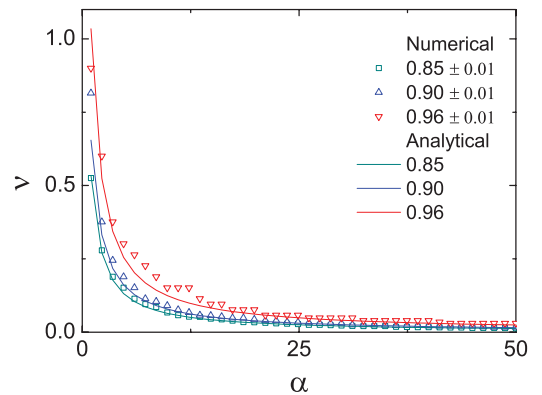


FIG. 2. (Color online) Threshold frequency on the widths of the zero-momentum Gaussian wave packet. The plots are Eq. (25) and numerical results corresponding to the average fidelities as  $0.96 \pm 0.01$ ,  $0.90 \pm 0.01$ , and  $0.85 \pm 0.01$ . It shows that the threshold frequency increases rapidly when the width of the state gets narrow.

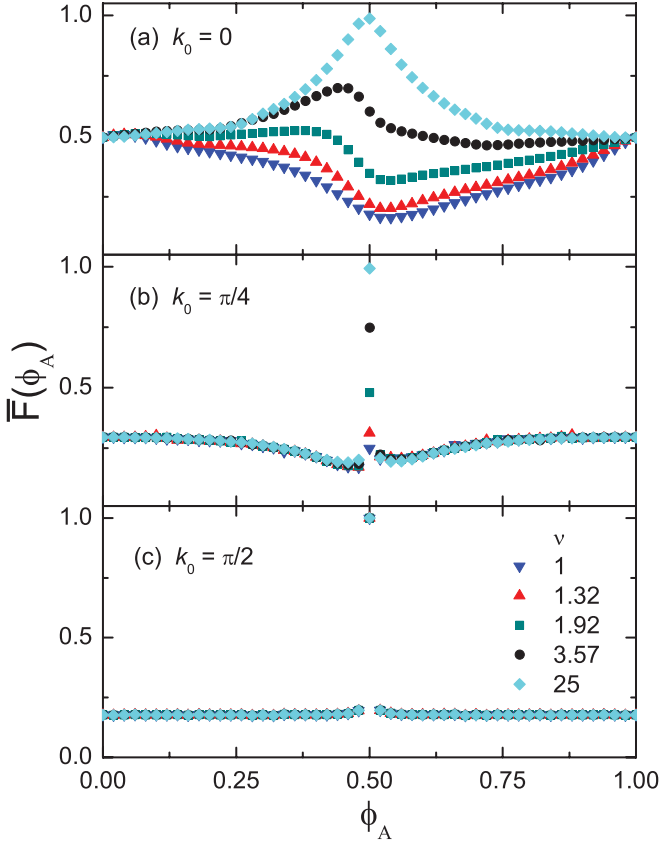


FIG. 3. (Color online) Average fidelity as a function of field amplitude  $\phi_A$  (units of  $\pi$ ) and frequency  $\nu$  (units of  $J$ ) of a square-wave flux for the Gaussian wave packet with  $\alpha = 50$  and central momenta  $k_0 = 0, \pi/4, \pi/2$  on an  $N = 1000$  ring. The average fidelity is computed over the time interval  $[0, 25N/J]$ . It shows that  $\pi/2$  is the optimal amplitude, and the fidelity becomes very sensitive to the magnitude for the initial wave packet with high speed.

First of all, we investigate the influence of the amplitude. The numerical simulations are performed in Fig. 3 for a Gaussian wave packet, which has the form of Eq. (23) with different central momenta in the systems with different amplitudes and different frequencies. It shows that the average fidelity approaches to unit for  $\phi_A = \pi/2$  when  $\nu$  is sufficiently high, which is in agreement with the above analysis. And it is noted that the locations of the maxima of the average fidelity for moderate  $\nu$  shift to the left for the case of  $k_0 = 0$ . This is important for practical implementation. In the case of insufficiently high frequency, the optimal amplitude should be smaller than  $\pi/2$ . For  $k_0 = \pi/4, \pi/2$ , the fidelity becomes very sensitive to the magnitude of  $\phi_A$ . This feature can be exploited to select the wave packet with preferable  $k_0$  in the following way. Suppose a many-particle initial state, which consists of wave packets with various speeds. One can first tune  $\phi_0$  to meet  $\phi_0 + k_0 = \pi/2$ . Then one can take  $\phi_A = \pi/2$  to hold the wave packets, with  $k_0$  on demand.

Second, the analysis above is based on the assumption that not only is the amplitude of the flux  $\pi/2$ , but the frequency is also sufficiently high. Then, even the amplitude is taken exactly as  $\pi/2$ ; the efficiency of the scheme is different for different quantum states under the finite frequency. For instance, the average fidelity during the period  $\tau$  mainly depends on the

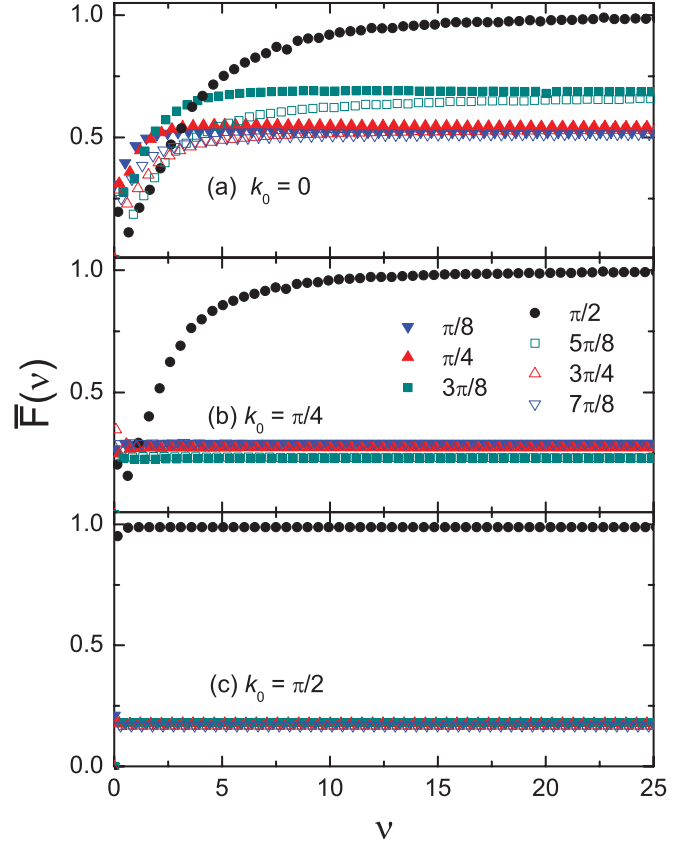


FIG. 4. (Color online) Average fidelity as a function of frequency of the square-wave flux for a Gaussian wave packet with  $\alpha = 50$  on an  $N = 1000$  ring. Panels stand for different values of the amplitudes,  $\phi_A = \pi/8, \pi/4, 3\pi/8, \pi/2, 5\pi/8, 3\pi/4, 7\pi/8$ , and central momenta,  $k_0 = 0, \pi/4, \pi/2$ , of the initial wave packet. It shows that when  $\phi_A = \pi/2$ , frequently alternating flux suppresses the evolution of the quantum states. Here the frequency  $\nu$  is expressed in units of  $J$ .

overlap of the initial wave packet and its evolution driven by  $H_{\pm}$ . In order to demonstrate these analyses, the numerical simulations are performed for two kinds of initial states: a Gaussian wave packet (GWP) with central momentum  $k_0$ , which has the form of Eq. (23), and the single-site state  $|l\rangle \equiv a_l^\dagger|0\rangle$ . We consider the time evolutions of this GWP with different  $k_0$  in the system with different amplitudes and different frequencies. The average fidelity  $\bar{F}(\tau)$  over the interval  $T \leq 25N/J$  is plotted in Fig. 4. It shows the following features: (i) The average fidelity approaches to unit for all of the given initial wave packets with different  $k_0$  when the amplitude is  $\pi/2$ , which is in agreement with the above analysis. (ii) The threshold frequency in the case of  $\phi_A = \pi/2$  gets lower as  $k_0$  goes closer to  $\pi/2$ . This is also in accordance with the above analysis. Actually, the velocity of a  $\pi/2$  wave packet becomes zero under the Hamiltonians  $H_{\pm}$ . Thus it deviates from the initial state slightly during the interval  $\tau$ , leading to a high fidelity. (iii) The optimal average fidelity becomes more sensitive as  $k_0$  goes closer to  $\pi/2$ , which is in agreement with the results in Fig. 3.

Based on these features, one can design a scheme to achieve the maximal fidelity. In the ideal case, for any given frequency of the field,  $\phi_A = \pi/2$  is always preferable. When

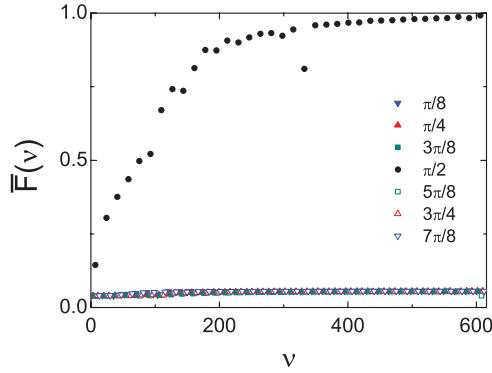


FIG. 5. (Color online) Average fidelity as a function of frequency of the square-wave flux for a single-site state on an  $N = 1000$  ring. Plots are presented for different values of the amplitudes,  $\phi_A = \pi/8, \pi/4, 3\pi/8, \pi/2, 5\pi/8, 3\pi/4$ , and  $7\pi/8$ . It shows that when  $\phi_A = \pi/2$ , frequently alternating flux suppresses the evolution of the quantum states, while other cases exhibit small fidelity. Here the frequency  $\nu$  is expressed in units of  $J$ .

the frequency is not sufficiently high, one can tune  $\phi_0$  to match  $k_0$  in order to achieve a lower threshold frequency. However, the accuracy of the field may affect the fidelity due to the sensitivity of it around  $\phi_A = \pi/2$  in practice. Then one can tune  $\phi_0$  to stabilize the fidelity.

Finally, in order to demonstrate the applicability of our findings to control a quantum state, we also plot the average fidelity for a single-site state  $|l\rangle \equiv a_l^\dagger|0\rangle$  in Fig. 5. Such a state has  $|c_k|^2 = 1/N$  and is the narrowest limit of a wave packet. It shows that the average fidelity approaches to unit only in the case of  $\phi_A = \pi/2$  and a relative high frequency. And to demonstrate the efficiency of this method, we take an initial zero-momentum Gaussian wave packet as examples. Numerical simulation is performed in Fig. 2 for the dependence of the threshold frequency on the widths for the given average fidelities. For a comparison, we draw the curves from Eq. (25) and numerical results corresponding to the average fidelities as  $0.96 \pm 0.01$ ,  $0.90 \pm 0.01$ , and  $0.85 \pm 0.01$ . The width coefficient  $\alpha$  of the wave packet is taken from 1 to 50, ranging from a single-site state to a very wide wave packet that is approximately a plane wave with zero momentum. As can be seen from the figure, analytical and numerical results both indicate that the threshold frequency increases rapidly when the width of the state gets narrow. Then for a finite-frequency field, such a scheme has a high efficiency for a broad wave packet.

#### IV. MONOCHROMATIC WAVE

The simplicity of the square-wave field makes it easy to make an analytical investigation for the problems of concern here because the exact solution of this model is helpful to clearly present the main idea of the scheme without involving much more complicated calculations. However, such a toy model is not exactly accessible in experiments due to the sudden change of the flux. In this section, we will consider the monochromatic-wave field, which is more practical. It will be shown analytically and numerically that both cases are similar qualitatively.

The monochromatic-wave field is in the form of

$$\phi(t) = \phi_0 + \phi_A \sin \omega t. \quad (26)$$

Unlike the square-wave field, even in the special case of  $\phi_A = \pi/2$ , the fidelity is no longer a periodic function due to the breaking of the time-reversal symmetry. Thus one should consider the integral to the whole time duration. However, the analytical function of  $\phi(t)$  may lead to some analytical results. Here we still neglect  $\phi_0$  for simplicity. We first investigate some special cases analytically to seek the optimal  $\phi_A$  satisfying the relation Eq. (18), and then perform numerical simulations for more general cases.

By considering the evolved state at the instant  $n\tau$ , where  $n$  is an integer, we have

$$\begin{aligned} f_k(n\tau) &= \int_0^{n\tau} \cos[k + \phi_A \sin \omega t'] dt' \\ &= n\tau \cos k \mathcal{J}_0(\phi_A). \end{aligned} \quad (27)$$

Here,

$$\mathcal{J}_m(x) = \frac{1}{\pi} \int_0^\pi \cos[m\theta - x \sin(\theta)] d\theta \quad (28)$$

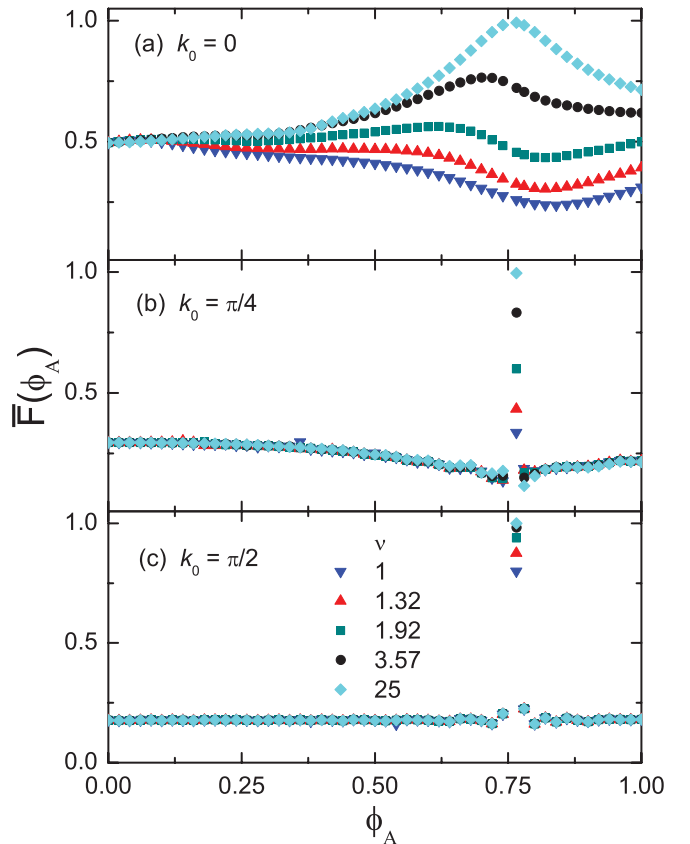


FIG. 6. (Color online) Average fidelity as a function of field amplitude  $\phi_A$  (units of  $\pi$ ) and frequency  $\nu$  (units of  $J$ ) of a monochromatic-wave flux for the Gaussian wave packet with  $\alpha = 50$  and central momenta  $k_0 = 0, \pi/4, \pi/2$ , on an  $N = 1000$  ring. The average fidelity is computed over the time interval  $[0, 25N/J]$ . It shows that  $0.765\pi$  is the optimal amplitude and the fidelity becomes very sensitive to the magnitude for the initial wave packet with high speed.



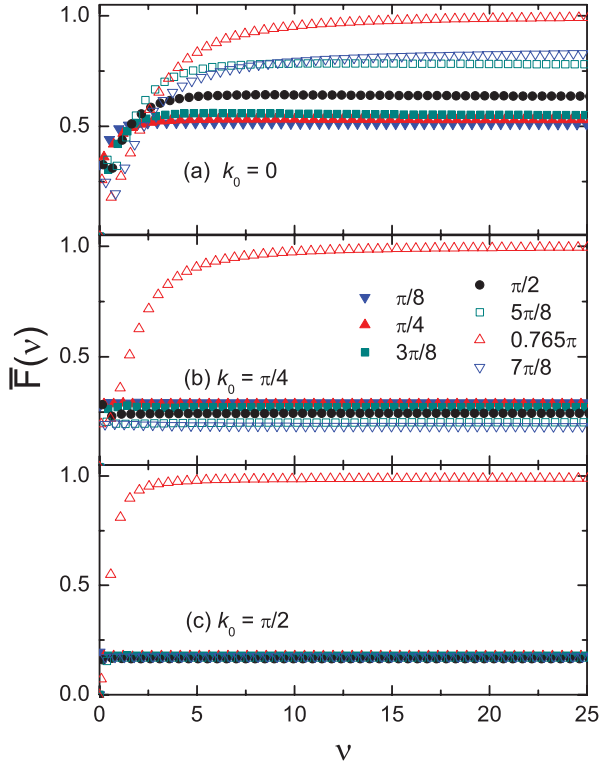


FIG. 7. (Color online) Average fidelity as a function of frequency of the monochromatic-wave flux for a Gaussian wave packet with  $\alpha = 50$  on an  $N = 1000$  ring. Panels stand for different values of the amplitudes,  $\phi_A = \pi/8, \pi/4, 3\pi/8, \pi/2, 5\pi/8, 0.765\pi, 7\pi/8$ , and central momenta,  $k_0 = 0, \pi/4, \pi/2$ , of the initial wave packet. It shows that when  $\phi_A = 0.765\pi$ , frequently alternating flux suppresses the evolution of the quantum states. Here the frequency  $\nu$  is expressed in units of  $J$ .

are the Bessel functions of the first kind. Then the corresponding fidelity is

$$F(n\tau) = \left| \sum_k |c_k|^2 e^{i2Jn\tau \cos k \mathcal{J}_0(\phi_A)} \right|. \quad (29)$$

Note that by taking  $\phi_A = 0.765\pi$ , we have  $\mathcal{J}_0(\phi_A) = 0$ , which leads to  $F(n\tau) = 1$  for an arbitrary initial state. This fact is quite similar to the case of the square-wave field with  $\phi_A = \pi/2$ .

Now we apply our numerical investigation to the more general cases. We perform the numerical simulations for the same states discussed in the last section. The numerical results are plotted in Figs. 6, 7, and 8. They show that the square and monochromatic waves lead to the similar result, but with different optimal  $\phi_A$ . The corresponding numerical result for the threshold frequency  $\nu_c(\alpha)$  as a function of the width of the wave packet is plotted in Fig. 9.

Based on the numerical results presented in the two above sections, we conclude that the evolution of a quantum state

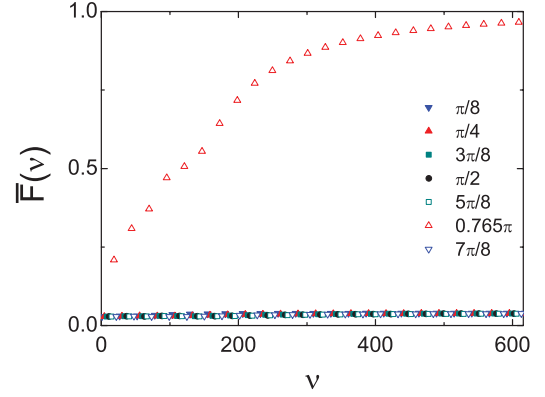


FIG. 8. (Color online) Average fidelity as a function of frequency of the monochromatic-wave flux for a single-site state on an  $N = 1000$  ring. Plots are presented for different values of the amplitudes,  $\phi_A = \pi/8, \pi/4, 3\pi/8, \pi/2, 5\pi/8, 0.765\pi$ , and  $7\pi/8$ . It shows that when  $\phi_A = 0.765\pi$ , frequently alternating flux suppresses the evolution of the quantum states, while other cases exhibit small fidelity. Here the frequency  $\nu$  is expressed in units of  $J$ .

can be suppressed through the time-periodic flux. In both situations, the efficiency of the schemes depends on the parameters  $\phi_A, \phi_0, \omega, k_0$ , and  $\alpha$  in a similar manner. The features can be exploited to control quantum dynamics for quantum-information and computation purposes.

## V. DISCUSSION

We have seen that the threaded magnetic flux, instead of the electric field, plays an important role in controlling a state. It can be applied to a more extended system to control an uncharged particle. Actually, if the system is rotated, an effective magnetic field will be induced in the rotating frame of references. Therefore, a neutral-particle state in a ring lattice can be controlled via torsional oscillation.

For a rotating ring with angular frequency  $\Omega$ , an additional term

$$H_R = -\Omega L_z = -\Omega K \sum_{j=1}^N (ia_j^\dagger a_{j+1} + \text{H.c.}) \quad (30)$$

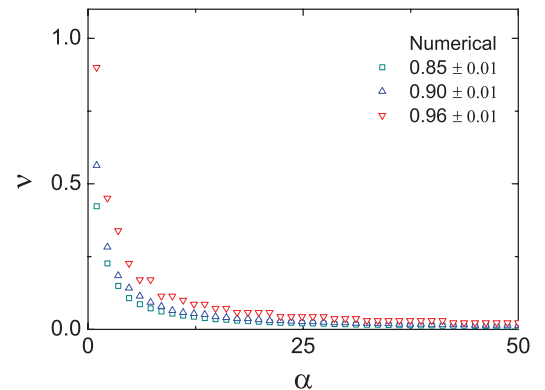


FIG. 9. (Color online) The same as Fig. 2, but with only the numerical result for the monochromatic-wave field.

should be added on the Hamiltonian with  $\phi = 0$  in the noninertial frame [18], where  $K$  is a constant that depends on the geometry of the ring.

In summary, we have studied the influence of periodically alternating magnetic fields on the dynamics of a quantum state on a tight-binding ring. Our analytical and numerical calculations indicate that the evolution of a quantum state can be suppressed through the time-periodic flux. The efficiency of the scheme depends on not only the system parameters  $\phi_A$ ,  $\phi_0$ , and  $\omega$ , but also the state parameters  $k_0$  and  $\alpha$ . Based on the features of the dynamics, one can choose an appropriate system to freeze a given state with an expected average fidelity. It can

also be exploited to select and hold a specific wave packet among the many-body particles, thus providing a means to perform the quantum-state engineering. We expect that such an observation has applications for information processing and quantum-device physics.

### ACKNOWLEDGMENTS

We acknowledge the support of the CNSF (Grant No. 10874091) and National Basic Research Program (973 Program) of China under Grant No. 2012CB921900.

- 
- [1] S. Bose, *Phys. Rev. Lett.* **91**, 207901 (2003).
  - [2] M. Christandl, N. Datta, A. Ekert, and A. J. Landahl, *Phys. Rev. Lett.* **92**, 187902 (2004).
  - [3] T. Shi, Y. Li, Z. Song, and C. P. Sun, *Phys. Rev. A* **71**, 032309 (2005).
  - [4] Y. Li, T. Shi, B. Chen, Z. Song, and C. P. Sun, *Phys. Rev. A* **71**, 022301 (2005).
  - [5] V. Subrahmanyam, *Phys. Rev. A* **69**, 034304 (2004).
  - [6] Z. Song and C. P. Sun, *Low Temp. Phys.* **31**, 686 (2005).
  - [7] T. J. Osborne and N. Linden, *Phys. Rev. A* **69**, 052315 (2004).
  - [8] M. F. Yanik and S. Fan, *Phys. Rev. Lett.* **92**, 083901 (2004).
  - [9] M. F. Yanik and S. Fan, *Phys. Rev. Lett.* **93**, 173903 (2004).
  - [10] M. F. Yanik, W. Suh, Z. Wang, and S. Fan, *Phys. Rev. Lett.* **93**, 233903 (2004).
  - [11] L. Zhou, Y. B. Gao, Z. Song, and C. P. Sun, *Phys. Rev. A* **77**, 013831 (2008).
  - [12] M. S. Byrd, L. A. Wu, and D. A. Lidar, *J. Mod. Opt.* **51**, 2449 (2004).
  - [13] C. Search and P. R. Berman, *Phys. Rev. Lett.* **85**, 2272 (2000).
  - [14] L. Zhou, S. Yang, Y. X. Liu, C. P. Sun, and F. Nori, *Phys. Rev. A* **80**, 062109 (2009).
  - [15] A. Eckardt, C. Weiss, and M. Holthaus, *Phys. Rev. Lett.* **95**, 260404 (2005); A. Eckardt and M. Holthaus, *Europhys. Lett.* **80**, 50004 (2007).
  - [16] H. Lignier, C. Sias, D. Ciampini, Y. Singh, A. Zenesini, O. Morsch, and E. Arimondo, *Phys. Rev. Lett.* **99**, 220403 (2007).
  - [17] S. Yang, Z. Song, and C. P. Sun, *Phys. Rev. A* **73**, 022317 (2006).
  - [18] R. Bhat, L. D. Carr, and M. J. Holland, *Phys. Rev. Lett.* **96**, 060405 (2006).